Academic Journal of Applied Mathematical Sciences
ISSN(e): 2415-2188, ISSN(p): 2415-5225
Vol. 6, Issue. 7, pp: 126-135, 2020
URL: https://arpgweb.com/journal/journal/17
DOI: https://doi.org/10.32861/ajams.67.126.135

Academic Research Publishing Group

Original Research **Open Access**

Time-Dependent Flow of a Couple Stress Fluid in an Elastic Circular Cylinder with Application to the Human Circulatory System

T. S. L. Radhika (Corresponding Author)
BITS Pilani- Hyderabad Campus, Hyderabad, India
Email: radhikatsl@hyderabad.bits-pilani.ac.in

T. Raja Rani
Military Technological College, Muscat, Oman

A. Karthik
BITS Pilani- Hyderabad Campus, Hyderabad, India

Article History
Received: June 23, 2020
Revised: July 21,2020
Accepted: July 25, 2020
Published: July 29, 2020

Abstract

In this paper, we developed a mathematical model for blood flow in the human circulatory system. This model presumes blood to be a couple stress fluid, its flow to be pulsatile, and the artery an elastic circular pipe whose radius is assumed to vary with transmural pressure. The governing differential equation for the flow velocity is time-dependent and has been solved using the homotopy perturbation method. This velocity has been used to estimate the elastic modulus E of the artery, which is a measure of its stiffness and an important metric used by clinical practitioners to understand the state of the cardiovascular system. In this work, the radial artery has been considered and a limited set of experimental data, available for four cases, has been taken from the published literature to validate the model. While the experimental values of elastic modulus reported in literature lie in the range 2.68 1.81 *MPa.s*, those estimated through the proposed model range from 3.05 to 5.98 *MPa.s*, appearing to be in close agreement.

Keywords: Couple stress fluid; Elastic tube; Pulsatile flow; Circulatory system; Transmural pressure; Homotopy perturbation method.

1. Introduction

The flow of a non-Newtonian fluid through an elastic pipe is a problem of interest in many sciences and engineering applications, particularly in biomedical engineering and more precisely in the study of the human circulatory system. It is well known that the important components of the human circulatory system are the heart that generates a pressure gradient required to drive blood to all parts of the body, and the arteries which carry blood to various organs. The main features of this system are as follows:

(i) Pulsatile pumping of the heart provides an arterial pressure that, under normal conditions, varies between 120 *mmHg* (systolic pressure) and 80 *mmHg* (diastolic pressure).
(ii) Arteries are elastic vessels with a complex geometry of curved pipes that includes tapering and branching.
(iii) Blood is a suspension containing red blood cells, white cells and platelets.

Several mathematical models have been proposed from time to time [1-9] to study the blood flow through arteries considering some (but not all) of the above features, such as the flow to be pulsatile, arteries to be elastic or blood to be a non-Newtonian fluid. While several physical parameters related to arteries, such as distensibility and compliance, could be determined, recent studies [10-13] have identified another important physical parameter known as 'arterial stiffness'. This parameter, related to the elastic (or elasticity) modulus of the artery (denoted by *E)*, is an important indicator of vascular changes that may eventually result in a major cardiovascular disease [14-17].

From basic principles of wave propagation in an elastic medium, it is known that the longitudinal wave velocity v in a fluid is related to the bulk elastic modulus K and density of the fluid ρ as: $v = \sqrt{\frac{K}{\rho}}$. It is clear that a higher value of K implies a higher velocity. This is because a higher value of the elasticity modulus implies a medium that is less elastic and stiffer, thus offering less resistance to the flow of the fluid and leading to its higher velocity. Applying this principle to the flow of blood through a human artery (treated as an elastic medium), it may easily be seen that the pulse wave velocity (PWV), arising out of the pulsatile nature of the flow, is a good measure of the arterial stiffness [18]. Since PWV is interrelated to the pulse transit time (PTT), it is possible to derive PWV by measuring PTT experimentally [19]. It may be mentioned that PTT is the time taken for the pressure pulse to flow from the point of origin to the periphery of the artery (in the longitudinal sense). Mathematical models have been proposed over the years to estimate the arterial stiffness by relating PWV to the elastic modulus of the artery [20-22]. However, very few of them relate the blood flow velocity (taken to be pulsatile) to the elastic modulus of the artery.

However, as mentioned earlier, these models assumed only one or at most two of the features mentioned above at a time to describe the blood flow in the human circulatory system. It may be noted that blood flow velocity is the rate at which blood moves through a particular artery, whereas PWV is the velocity at which the pressure pulse propagates through the same artery.

Thus in the current work, we introduce a new method to estimate *E* using the blood flow velocity while also including almost all main features of the human circulatory system. That is blood flow under a pulsatile pressure gradient, the non-Newtonian nature of the blood, and the elastic nature of the artery. We assume the tube to be non-curved, which is indeed a realistic assumption in modelling blood flow through a single non-branching artery (such as the radial artery, which is a major artery present in the human forearm) that has been taken up in our present study. We have chosen to work on this artery since the data necessary for the verification of our proposed mathematical model are available for this artery in the literature.

An outline of the proposed model is as follows. The elastic nature of the artery is as given in equation (12), where the radius of the artery at a given point is taken to be a linear function of the transmural pressure at that point. Blood flow is considered to be driven by a pulsatile pressure gradient, as described in equation (11). Blood itself is modelled as a non-Newtonian fluid described by the couple stress fluid model. This couple stress fluid model which was shown to be the simplest generalisation of the classical fluid theory describes an important physical concept in fluids called couple stresses that the classical fluid theory ignores [23-25].

Figure-1. An illustration of (a) the stress and (b) the couple stress distribution in the cylindrical geometry

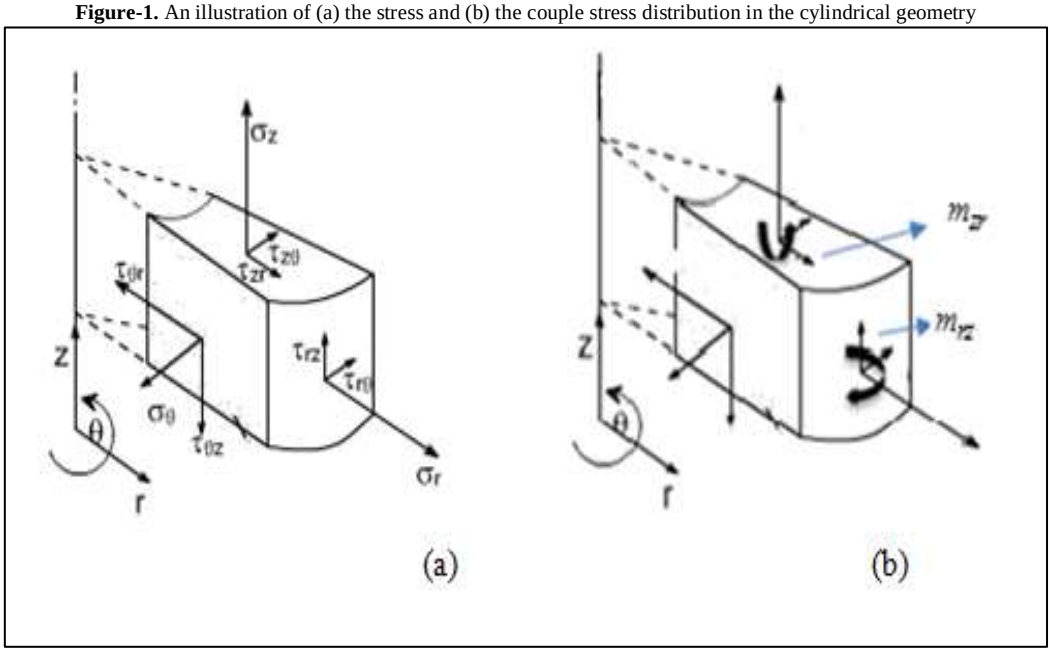

In Figure 1, we depict the stress and couple stress components acting on an elemental volume of the fluid in the cylindrical polar coordinate system, where θ is measured in the plane perpendicular to the *z*-axis. In Figure 1(a), $\tau_{rz}, \tau_{zr}, \tau_{\theta z}, \tau_{z\theta}, \tau_{r\theta}, \tau_{\theta r}$ denote the tangential stress components and $\sigma_r, \sigma_\theta, \sigma_z$ denote the normal stress components of the stress tensor. In Figure 1(b), m_{rz} denotes the *z*- component of the couple stress vector on the plane $r = \text{constant}$ (indicated by the curl), and m_{zr} is the *r*-component of the couple stress vector on the plane $z = \text{constant}$ (indicated again by the curl). Similar interpretations can be given for the other couple stress components. We shall see later (section 2) that out of these 18 (9 stress + 9 couple stress) components, the present formulation results in only four nonzero components (two stress components: τ_{rz} and τ_{zr}, and two couple stress components: m_{rz} and m_{zr}).

This couple stress model contains two parameters, known respectively as the couple stress viscosity, indicated by μ, material parameter σ, and the momentum, denoted by η_1 [24, 25]. This model, when fitted to the experimental data available in the literature [23, 26-28] and shown in Table 1, will help in determining the values of these parameters.

Table-1. Experimental data relevant to the model for four cases [23]

Parameter	Case 1	Case 2	Case 3	Case 4
Age (years)	27	28	25	48
Height (*cm*)	174	173	175	152.4
PTT (*ms*)	244	275	205	205
PWV (*m/s*)	4.28	3.77	5.12	4.46
BP (Blood Pressure) (sys/dias) *mmHg*	115/67	108/82	125/82	140/90
Heart Rate/min	57	96	73	90

After determining the values of these parameters, the flow variables present in the model have been evaluated, and an estimate for the elastic modulus of the radial artery has been arrived at using the methodology described in Section 4.

We have observed that under similar conditions, the values for E obtained using the present model agreed with those of the 'Constant Viscosity' model [21]. The next step of our research would be to use the present model under different physical conditions (namely curved artery, branching arteries, etc.), in which case this method is expected to be more appropriate than the Constant Viscosity model because it incorporates more realistic physical features.

2. Mathematical Formulation of the Problem

Let us consider an unsteady (time-dependent) flow of a fluid (blood in our case) in an elastic circular tube mimicking the radial artery (Figure 2), and whose radius is assumed to vary linearly with the transmural pressure (pressure difference across the arterial wall, Figure 3) along the tube. We consider the cylindrical polar coordinate system (r,θ,z) (where r and z are the radial and axial coordinates, respectively, and θ is the azimuthal angle) to describe the geometry of the problem and assume the fluid flow to be in the z-direction as shown in Figure 2.

Figure 2. A schematic of fluid flow in an elastic tube [21]

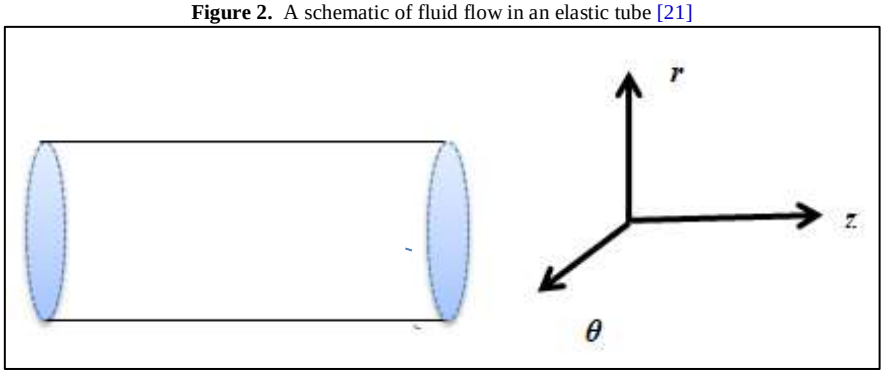

Figure-3. Illustration of transmural pressure across the arterial wall [26]

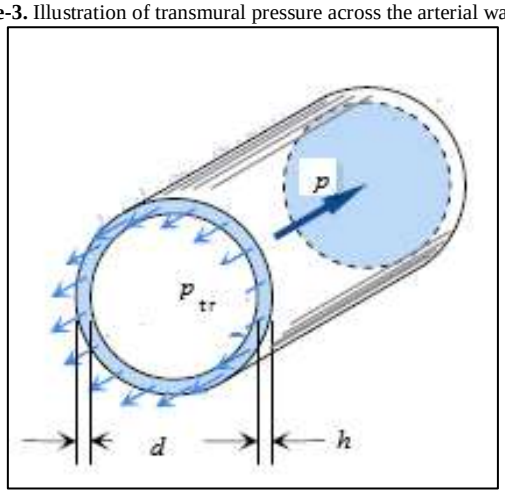

(p is the thermodynamic pressure (acting along the longitudinal direction), p_{tr} is the transmural pressure (across the wall, i.e. perpendicular to the wall), d is the diameter of the tube and h is the wall thickness. Arrows indicate the direction in which these pressures are to be considered.)

The fluid is considered to be incompressible, and the tube is taken to be of infinite length. We also assume that the flow is axisymmetric so that the components of the velocity ($\overline{q}$) and the thermodynamic pressure, denoted by p,

are functions only of *r*, *z* and time *t*. Also, the velocity vector $\bar{q}(r,z,t)=\left(u(r,z,t),0,w(r,z,t)\right)$ (where $u(r,z,t)$ (or q_r), $w(r,z,t)$ (or q_z) are scalar functions) and the thermodynamic pressure *p* is a function $p(r,z,t)$.

The equations of motion governing the couple stress fluid flow are [23-25]:

$$\frac{\partial\rho}{\partial t}+\rho div(\bar{q})=0, \tag{1}$$

$$\rho\frac{d\bar{q}}{dt}=-\nabla p+\rho\,\bar{f}+\frac{1}{2}curl\left(\rho\,\bar{c}\right)+div\left(\tau^{(s)}\right)+\frac{1}{2}curl(div(m)), \tag{2}$$

where $\vec{f}$ is the body force per unit mass and $\bar{c}$ is body moment per unit mass.

In this work, we assume that body forces and body couple are absent, and thus the vectors $\bar{f}$ and $\bar{c}$ are identically zero. This can be justified by the fact that body forces and body couple arise due to external forces, such as gravitational force or centrifugal force, which even if present, are assumed to have a negligible effect on the blood flow through the arteries.

Further, for incompressible flows (for which ρ is independent of time), equation (1) reduces to

$$div(\bar{q})=0. \tag{3}$$

Thus, with the assumptions mentioned above, equation (2) takes the form:

$$\rho\frac{d\bar{q}}{dt}=-\nabla p+\mu\nabla^2\bar{q}-\eta_1\nabla^4\bar{q}. \tag{4}$$

Further, since $\bar{q}(r,z,t)=\left(u(r,z,t),0,w(r,z,t)\right)$, the equation of continuity (3) further reduces to

$$\frac{\partial u}{\partial r}+\frac{u}{r}+\frac{\partial w}{\partial z}=0. \tag{5}$$

Also, under the assumption that the radial component of the flow velocity and the convective acceleration terms are respectively of a smaller order of magnitude with respect to the axial flow velocity and the local acceleration terms, the momentum equation given in (7) reduces to

$$r\text{-direction}: \quad -\frac{\partial p}{\partial r}=0, \tag{6}$$

z-direction :

$$\rho\left(\frac{\partial w}{\partial t}+u\frac{\partial w}{\partial r}+w\frac{\partial w}{\partial z}\right)=-\frac{\partial p}{\partial z}+\mu\left(\frac{\partial^2 w}{\partial r^2}+\frac{1}{r}\frac{\partial w}{\partial r}\right)-\eta_1\left(\frac{\partial^4 w}{\partial r^4}+\frac{2}{r}\frac{\partial^3 w}{\partial r^3}-\frac{1}{r^2}\frac{\partial^2 w}{\partial r^2}+\frac{1}{r^3}\frac{\partial w}{\partial r}\right), \tag{7}$$

where μ is the couple stress viscosity in *Pa.s*, η_1 is the momentum in *kg.m.s*$^{-1}$, and *p* is the fluid (blood) pressure whose gradient, in view of the pulsatile nature of the flow is assumed to take the form Burton [29]

$$-\frac{\partial p}{\partial z}=a_0+a_1\cos\omega t, t\geq 0, \tag{8}$$

where a_0 and a_1 are respectively the constant amplitude and amplitude of the pulsatile component of the pressure gradient (*Pa. m*$^{-1}$), and $\omega=2\pi f$, f is the number of heartbeats per minute.

Further, the tube (artery) is assumed to be elastic, with its radius $R(z)$ varying linearly with the local transmural pressure $p_{tr}(z)$ according to

$$R(z)=R_0\left(1+\alpha p_{tr}(z)\right), \tag{9}$$

where α is a flexibility coefficient, and R_0 is the radius of the tube when $p_{tr}(z)$ is zero [20]. It may be noted that, while in reality, the radius of the artery is a function of both *z* and *t*, it has been modelled as a constant, since calculations in our model are restricted to one cardiac cycle.

Boundary conditions: For the present problem, we assume a no-slip boundary condition, meaning the flow velocity is zero on the periphery of the artery (in the radial sense). From the theory proposed by Aero, *et al.* [30], the couple stresses on the boundary are proportional to the difference between the micro-rotation of the fluid particles and the angular velocity of the fluid flow at the boundary. The proportionality constant of this relationship is termed as the friction factor, which represents the fluid wall friction and is considered to be zero in the current context. Also, we assume that the velocity is finite at the centre of the tube.

Thus, the mathematical representation of the boundary conditions can be given as,

(i) $u = 0, w = 0$ on $r = R(z)$ (no-slip boundary condition), (10)

(ii) $\frac{\partial^2 w}{\partial r^2} - \frac{\sigma}{r}\frac{\partial w}{\partial r} = 0$ on $r = R(z)$ (couple stresses vanish on the wall), with $\sigma = \frac{\eta_1'}{\eta_1}$, (11)

(iii) $\frac{\partial^2 w}{\partial r^2} - \frac{\sigma}{r}\frac{\partial w}{\partial r}$ is finite at $r = 0$, (12)

(iv) $\frac{\partial w}{\partial r} = 0$ at $r = 0$ (velocity is finite at the centre of the tube). (13)

Since equation (10) is a time-dependent partial differential equation (time-dependent PDE), it is required to have an initial condition. One form of the condition (solution) would be to take the radial velocity component to be zero, i.e., $u(r,z,t) = 0$ and derive an expression for the axial velocity component, i.e. $w(r,z,t)$ satisfying equations (5) and (7) together with the boundary conditions given in (10)-(13).

In view of our assumption that the radial component of the velocity is zero, equation (8) reduces to

$$\frac{\partial w}{\partial z} = 0. \tag{14}$$

Thus $w(r,z,t)$ is independent of z. The steady-state problem can now be re-written as

$$\nabla^4 w(r,0) - \frac{\mu}{\eta_1}\nabla^2 w(r,0) = \frac{1}{\eta_1}\left(\frac{\partial p}{\partial z}\right), \tag{15}$$

where $\nabla^2 \equiv \frac{\partial^2}{\partial r^2} + \frac{1}{r}\frac{\partial}{\partial r}$, (16)

which is solved using the method of undetermined coefficients presented in Appendix A. The solution is presented below as:

$$w(r,0) = \frac{1}{4\mu}\left(\frac{\partial p}{\partial z}\right)_{t=0}\left(1 - \frac{r^2}{R_0^2}\right)R_0^2 + \frac{1}{2\mu}\left(\frac{\partial p}{\partial z}\right)_{t=0}(1-\sigma)\frac{I_0\left(\sqrt{\frac{\mu}{\eta_1}}r\right) - I_0\left(\sqrt{\frac{\mu}{\eta_1}}R_0\right)}{\frac{\mu}{\eta_1}I_0''\left(\sqrt{\frac{\mu}{\eta_1}}R_0\right) - \frac{\sigma}{R_0}\sqrt{\frac{\mu}{\eta_1}}I_0'\left(\sqrt{\frac{\mu}{\eta_1}}R_0\right)}, \tag{17}$$

where $I_0(r)$ is the modified Bessel function of the first kind and order zero, and $I_0'(r)$ and $I_0''(r)$ are its first and second-order derivatives respectively (with respect to *r*) [31].

Finally, equations (5) and (7) are solved together with the conditions given in (10)-(13) and (17) using the homotopy perturbation method [32, 33].

3. Solution to the Problem

The system of partial differential equations (5) and (7) together with the initial and boundary conditions given in (10)-(13) is solved using the homotopy perturbation method (HPM), an elegant method to solve non-linear equations [32, 33]. According to this method, we assume the solutions of the system to be of the form:

$$u(r,z,t) = u_0(r,z,t) + pu_1(r,z,t) + p^2u_2(r,z,t) + \ldots,$$
$$w(r,z,t) = w_0(r,z,t) + pw_1(r,z,t) + p^2w_2(r,z,t) + \ldots \tag{18}$$

Here, the initial approximations are taken as $u_0(r,z,t) = 0$, $w_0(r,z,t) = w(r,0)$, given in expression (17). The subsequent approximations for $u(r,z,t)$ and $w(r,z,t)$ are found by defining homotopy functions as,

$$H_1(p) = (1-p)\left(\frac{\partial u}{\partial r} - \frac{\partial u_0}{\partial r}\right) + p\left(\frac{\partial u}{\partial r} + \frac{u}{r} + \frac{\partial w}{\partial z}\right), \text{ for equation (5)} \tag{19}$$

and that for equation (7) is defined as

$$H_2(p) = (1-p)\left(\frac{1}{r^4}\frac{\partial^4 w}{\partial r^4} - \frac{1}{r^4}\frac{\partial^4 w_0}{\partial r^4}\right) + p\left(\begin{array}{l}\rho\left(\frac{\partial w}{\partial t} + u\frac{\partial w}{\partial r} + w\frac{\partial w}{\partial z}\right) + \frac{\partial p}{\partial z} - \mu\left(\frac{1}{r}\frac{\partial w}{\partial r} + \frac{\partial^2 w}{\partial r^2}\right) \\ +\eta_1\left(\frac{\partial^4 w}{\partial r^4} + \frac{2}{r}\frac{\partial^3 w}{\partial r^3} - \frac{1}{r^2}\frac{\partial^2 w}{\partial r^2} + \frac{1}{r^3}\frac{\partial w}{\partial r}\right)\end{array}\right). \tag{20}$$

Comparing the coefficient of *p*, we get the equations governing $u_1(r,z,t)$ and $w_1(r,z,t)$ as

$$\frac{\partial u_1}{\partial r} = -\left(\frac{\partial w_0}{\partial z} + \frac{u_0}{r}\right), \tag{21}$$

$$\frac{\partial^4 w_1}{\partial r^4} = -r^4 \left(\begin{array}{l} \frac{\partial p}{\partial z} + \rho\left(\frac{\partial w_0}{\partial t} + u_0 \frac{\partial w_0}{\partial r} + w_0 \frac{\partial w_0}{\partial z}\right) - \\ \mu\left(\frac{\partial^2 w_0}{\partial r^2} + \frac{1}{r}\frac{\partial w_0}{\partial r} + \frac{1}{r^2}\frac{\partial^2 w_0}{\partial z^2}\right) - \eta_1\left(\frac{\partial^4 w_0}{\partial r^4} - \frac{2}{r}\frac{\partial^3 w_0}{\partial r^3} + \frac{1}{r^2}\frac{\partial^2 w_0}{\partial r^2} + \frac{1}{r^3}\frac{\partial w_0}{\partial r}\right) \end{array} \right). \tag{22}$$

And the conditions are $u_1 = 0$ on $r = R(z)$, $w_1 = 0$ on $r = R(z)$, $\frac{\partial^2 w_1}{\partial r^2} - \frac{\sigma}{r}\frac{\partial w_1}{\partial r} = 0$ on $r = R(z)$, $\frac{\partial^2 w_1}{\partial r^2} - \frac{\sigma}{r}\frac{\partial w_1}{\partial r}$ is finite at $r = 0$, $\frac{\partial w_1}{\partial r} = 0$ at $r = 0$ (23)

Solving these equations, we get expressions for the first approximation of the velocity components. Similarly, the coefficient of p^2 and higher powers have been collected to find the next approximations.

4. Methodology

- Calculate the volumetric flow rate *Q* given by

$Q = l \int_0^{R(z)} 2\pi r w(r, z, t) dr$, *l* is the length of the artery.

- Estimate *CO* as given by

$CO = \int_0^T Q dt$, where *T* is the pulse transit time, and *CO* represents the volume of the blood flowing in the radial artery.

- Determine the flexibility coefficient α (see expression (9)) by equating *CO* estimated above (which is a polynomial in α obtained by approximating the Bessel functions in expression (17) as polynomials in *x* [31]) to the cardiac output (2.6% of cardiac output (for a given case; the average value of 5.5*lt/min* is considered) for a radial artery [26]. The method for computation of *α* is mentioned in detail in Section 5.1.

- It may be pertinent to mention here that the cardiac output is the total volume of blood pumped by the heart per unit time.

- Calculate the average value (over one cardiac cycle) of $R(z)$, denoted by R_{avg}, by substituting the value of α and transmural pressure from Table 2 in expression (12) for all the four cases.

- Estimate the average value (over one cardiac cycle) of the stretch ratio of the radial artery, denoted by λ_{avg} and defined as

$$\lambda_{avg} = \frac{R_{avg}}{r_0},$$

where r_0 is the nominal radius of the artery as mentioned earlier.

- Find the circumferential stress by the formula [20]:

$$T_{circum} = \frac{\left(functional\ mean\ pressure\right) \times \left(average\ radius\ of\ the\ artery\right)}{wall\ thickness\ of\ the\ artery},$$

where the functional mean pressure is the mean pressure of the fluid in the artery.

Finally, estimate the average value (over one cardiac cycle) of the elastic modulus *E* of the artery using the formula [20]:

$$T_{circum} = E\left(\lambda_{avg} - 1\right).$$

5. Results and Discussion

In order to verify the validity of the proposed model, data related to four cases have been taken from the published literature [23], as shown in Table 1. Also, properties of blood and the dimensions of the radial artery have been extracted from the literature [20, 22, 26, 27] as shown in Table 2. The methodology introduced above has been applied to this data to obtain parameters of interest, as illustrated in Table 3.

Table-2. Physical properties of blood and the radial artery

Density of blood ρ (*kg/m*^{3})	1050 [20, 22]
Nominal Radius of radial artery r_0 (*mm*)	1.6 [27]
Wall thickness of radial artery *h* (*mm*)	0.28 [27]
Nominal transmural pressure $p_{tr}(z)$ (*kPas*)	11 [26]
Viscosity of blood μ (*Pas*)	0.004 [20, 22]
Stroke volume (*ml*/ beat)	60-130 [26]

Table-3. Fluid parameters and the arterial stiffness estimated using the proposed model

Parameter	**Case 1**	**Case 2**	**Case 3**	**Case 4**
a_0 (*Pa. m*$^{-1}$)	10597.6	11643.4	12841.2	15549.7
a_1 (*Pa. m*$^{-1}$)	6128.74	3338.92	5731.9	7288.93
Flexibility coefficient α (*Pa*$^{-1}$)	2.13×10^{-6}	1.63×10^{-6}	2.18×10^{-6}	1.23×10^{-6}
Average radius of the artery R_{avg} (*mm*)	1.625	1.629	1.638	1.622
$\sqrt{\eta_1 / \mu}$	5.82×10^{-6}	5.97×10^{-6}	5.53×10^{-6}	5.47×10^{-6}
σ	0.6	0.5	0.95	0.7
Circumferential stress T_{circum} (*kPa*)	63.22	69.062	73.39	81.25
E (*MPas*)	3.93	3.84	3.05	5.98

The constant and pulsatile components of the pressure gradient given in Table 3 (a_0 and a_1, respectively) have been estimated (using data from Table 1) for each case using the systolic (*sys*) and diastolic (*Dias*) components of their respective blood pressures (BP) as in [31]:

$a_0 = \left(\frac{1}{3}sys + \frac{2}{3}dias\right)/l,\quad a_1 = (sys - dias)/l,$ where *l* is the approximate length of the radial artery, estimated using the formula $l = 0.6\times \text{height of the individual}$ [34].

5.1. Computation of the Various Parameters in the Model to Estimate *E*

The methodology described earlier in Section 4 has been used to estimate the arterial stiffness parameter *E* for each of the cases mentioned in Table 1. We used approximate analytical methods (homotopy perturbation method in the present case) and numerical methods for computing the required flow variables and parameters in the model. We see from the expression (17) for the velocity of blood flow that it involves Bessel functions as well as its derivatives. We have used ascending series approximations (of degree 14) to these functions and thereby computed the velocity $w(r,z,t)$ [31]. Subsequently, the volumetric flow rate *Q* and *CO*, which are now polynomial functions in terms of the parameter α, are determined.

The value of the parameter α is found by solving the polynomial equation for *CO* using MATHEMATICA software [35]. Since this equation may result in multiple real solutions, an appropriate value for α has been chosen such that the values of the average radius R_{avg} predicted for each case do not deviate much from the experimental values reported in the literature [27, 28]. In doing so, the values of the couple stress fluid parameters μ , σ and η_1 have also been fixed (Table 3). This is not straight forward, however, since the values assigned to these parameters need to satisfy the inequalities mentioned in (3) and also lead to realistic values of the radius of the artery that are consistent with the published data. Subsequently, the average stretch ratio (λ_{avg}) and the circumferential stress (T_{Circum}) have been calculated before finally estimating the average elastic modulus *E* for each of the four cases.

Table-4. A comparison of values for *E* predicted by various Models

	Inviscid model [21]	**Constant Viscosity model [21]**	**Present (couple stress) Model**
Case 1	219.8 *kPa.s*	3.44 *MPa.s*	3.93*MPa.s*
Case 2	170.5 *kPa.s*	2.67 *MPa.s*	3.84*MPa.s*
Case 3	314.57 *kPa.s*	4.93 *MPa.s*	3.05*MPa.s*
Case 4	238.69 *kPa.s*	3.74 *MPa.s*	5.98*MPa.s*

Table 4 provides a comparison of values for the elastic modulus *E* predicted by various models for each of the cases. The inviscid model mentioned in the Table assumes the blood to be a Newtonian fluid with zero viscosity while the constant viscosity model, as the name implies, considers the blood to be of constant viscosity while still being a Newtonian fluid. However, as we mentioned earlier, the couple stress model in the present work assumes blood to be non-Newtonian described by the parameters μ, σ and η_1.

The experimental values for the elastic modulus E of the radial artery in humans have been reported to be of the order, 2.68±1.81 *MPa.s* [23]. This range of values appears to be more in agreement with those predicted by the constant viscosity model and the proposed couple stress model than by the inviscid model. While the constant viscosity model appears to predict a value similar to that by the couple stress model, we wish to mention that the artery under consideration for both models is the radial artery, with the assumption that it is straight. Thus, it is not surprising that both models predict the values of a similar order. It should, however, be mentioned that in case the arteries are curved and have to branch, the non-Newtonian nature of the fluid is expected to be predominant [36], and thus, the couple stress fluid might provide better estimates of E than the constant viscosity model. This aspect, however, needs further investigation.

6. Conclusion

In the present study, we proposed a model to estimate the elastic modulus E of the radial artery, assuming blood to be a non-Newtonian fluid, the artery to be a non-curved elastic tube, and the flow to be pulsatile. A small set of experimental data related to the radial artery for four individual cases has been used to estimate E using the model developed. Results indicate that these estimates of E are in broad agreement with the experimentally measured values reported in the literature. It should, however, be mentioned that the sample size used in the present work is very small, and some of the data on the arteries has been taken from the literature. Thus, more experimental data for a large number of cases is required before we can fully validate the model.

References

[1] David, N., 1997. "Ku: Blood flow in arteries." *Annu. Rev. Fluid Mech.*, vol. 29, pp. 399–434.

[2] Hellums, J. D., 1994. "Whitaker lecture: Biorheology in thrombosis research." *Ann. Biomed. Eng.*, vol. 22, pp. 445–455. Available: https://doi.org/10.1007/BF02367081

[3] Josip, T., 2005. *Suncica canic and andro mikeli: Effective model of the fluid flow through an elastic tube with variable radius*. Grazer Math. Ber., pp. 1-22.

[4] Lance, J. M. and Wayne, L. C., 2001. "Analytical solution for pulsatile axial flow velocity waveforms in curved elastic tubes." *IEEE Transactions On Biomedical Engineering*, vol. 48, pp. 864-873.

[5] Mette, S. O., Charles, S. P., Won, Y. K., Erik, M. P., Ali, N., and Jesper, L., 2000. "Numerical simulation and experimental validation of blood flow in arteries with structured-tree outflow conditions." *Annals of Biomedical Engineering*, vol. 28, pp. 1281–1299.

[6] Nidhi, V. and Parihar, R. S., 2010. "Mathematical model of blood flow through a tapered artery with mild stenosis and Hematocrit." *Journal of Modern Mathematics and Statistics*, vol. 4, pp. 38-43.

[7] Peskin, C. S. and McQueen, D., 1989. "A three-dimensional computational method for blood flow in the heart. I. Immersed elastic fibres in a viscous incompressible fluid." *J. Comput. Phys.*, vol. 81, pp. 372–405.

[8] Womersley, J. R., 1955. "Method for the calculation of velocity, rate of flow and viscous drag in arteries when their pressure gradient is known." *J. Physiol.*, vol. 127, pp. 553–63.

[9] He, X. and Ku, D. N., 1996. "Pulsatile flow in the human left coronary artery bifurcation: average conditions." *J. Biomech. Eng.*, vol. 118, pp. 74–82.

[10] Gamble, G., Zorn, J., Sanders, G., MacMahon, S., and Sharpe, N., 1994. "Estimation of arterial stiffness, compliance, and distensibility from M-mode ultrasound measurements of the common carotid artery, Stroke." *Journal of the American Heart Association*, vol. 25, pp. 11-16.

[11] Liao, D., Arnett, D. K., and Tyroler, H. A., 1999. "Arterial stiffness and the development of hypertension. The ARIC study." *Hypertension*, vol. 34, pp. 201-206.

[12] Marina, C. and Phil, C., 2012. "Role of arterial stiffness in cardiovascular disease." *J. R. Soc. Med. Cardiovasc. Dis.*, vol. 1, Available: https://pubmed.ncbi.nlm.nih.gov/24175067/

[13] Miodrag, J., Mojca, L., and Mišo, Š., 2014. *Arterial Stiffness and Cardiovascular Therapy*. Hindawi Publishing Corporation, pp. 1-11.

[14] Fung, P., Dumont, G., Ries, C., Mott, C., and Ansermino, M., 2004. "Continuous noninvasive blood pressure measurement by pulse transit time." In *Proceedings of the 26th Annual International Conference of the IEEE EMBS, San Francisco, CA, USA.*

[15] Hasegawa, H. and Kanai, H., 2004. "Measurement of elastic moduli of the arterial wall at multiple frequencies by remote actuation for assessment of viscoelasticity." *Japanese Journal of Applied Physics*, vol. 43, pp. 3197–3203.

[16] Stephane, A., Jonathan, M., and Huntley, R. C., 2008. "Characterization of wall stiffness in a blood vessel using cine-PC-MRI." In *Proceedings of the XI International Congress and Exposition on Experimental and Applied Mechanics, Orlando, Florida, USA.*

[17] Surya, P. B., Adam, G. C., James, M. W., Hrudaya, N., Jubal, R. W., John, R. C., and Mark, T. D., 2014. *Determinants of arterial stiffness in COPD*. BMC Pulmonary Medicine.

[18] Lee, S., Joanna, M. Y., and Simon, F., 2012. "Assessments of arterial stiffness and endothelial function using pulse wave analysis." *International Journal of Vascular Medicine*, Available: https://www.hindawi.com/journals/ijvm/2012/903107/

[19] Ye, S. Y., Kim, G. R., Jung, D. K., Baik, S. W., and Jeon, G. R., 2010. "Estimation of systolic and diastolic pressure using the pulse transit time." *World Academy of Science, Engineering and Technology*, vol. 43, pp. 726-731.

[20] Fung, Y. C., 1993. *Biomechanics- mechanical properties of living tissues*. 2nd ed. Springer.

[21] Mazumdar, J. N., 2004. *Bio-fluid mechanics*. Singapore: World Scientific Publishing.

[22] Myer, K., 2003. *Standard handbook of biomedical engineering and design*. TATA Mc: Graw Hill.

[23] Radhika, T. S. L. and Srinivas, M. B., 2014. "Evaluation of Mathematical models for estimation of arterial stiffness through pulse transit time measurement." In *IEEE Health care Innovations, Point- of- Care technology conference, Seattle, USA.*

[24] Stokes, V. K., 1971. "Effects of couple stresses in fluids on the creeping flow past a sphere." *Phy. Fluids.*, vol. 14, pp. 1580-1582.

[25] Stokes, V. K., 1984. *Theory of fluids with microstructure – An introduction*. Springer Verlag.

[26] Available: https://www3.nd.edu_nsl/Lectures/mphysics/MedicalPhysics/PartI.PhysicsoftheBody/Chapter3.PressureSystemoftheBody/3.2Physicsofthecardiovascularsystem/Physicsofthecardiovascularsystem.pdf

[27] Laurent, S., Girerd, X., Mourad, J. J., Lacolley, P., Beck, L., Boutouyrie, P., Mignot, J. P., and Safar, M., 1994. "Elastic modulus of the radial artery wall material is not increased in patients with essential hypertension, arteriosclerosis, thrombosis and vascular biology." *Journal of American Heart Association*, vol. 14, pp. 1223-1231.

[28] Michael, F., O'Rourke, J. A., Staessen, C. V., Daniel, D., and Ge´ rard, E. P., 2002. "Clinical applications of arterial stiffness." *Definitions and Reference Values, AJH*, vol. 15, pp. 426–444.

[29] Burton, A. C., 1966. *Physiology and biophysics of the circulation, introductory text*. Chicago: Year Book Medical Publisher.

[30] Aero, E. L., Bulygin, A. N., and Kuvshinskii, E. V., 1965. "Asymmetric hydromechanics." *Appl. Math. Mech.*, vol. 29, p. 333.

[31] Abramowitz, M. and Stegun, I. A., 1965. *Handbook of Mathematical functions with formulas, graphs and mathematical tables*. NewYork: Dover publications, INC.

[32] He, J. H., 2003. "Homotopy perturbation method, A new nonlinear analytic technique." *Appl. Math. Comput.*, vol. 135, pp. 73-79.

[33] He, J. H., 1999. "He Homotopy perturbation technique." *Computer Methods in Applied Mechanics and Engineering*, vol. 178, pp. 257-262.

[34] Avinash, S. V., Radhika, T. S. L., Srinivas, M. B., and Mannan, M., 2014. "Estimation of Arterial Stiffness through pulse transit time measurement." In *BIODEVICES 2014 - International Conference on Biomedical Electronics and Devices*. pp. 238-242.

[35] Stephen, W., 1996. *The Mathematica book*. 3rd ed. New York: Cambridge University Press.

[36] Gijsen, F. J. H., Vandevosse, F. N., and Janssen, J. D., 1999. "The influence of the non-Newtonian properties of blood on the flow in large arteries: Steady flow in a carotid bifurcation model." *J. Biomech.*, vol. 32, pp. 601-608.

Appendix A

Consider equation (19) given by

$$\nabla^4 w(r,0) - \frac{\mu}{\eta_1}\nabla^2 w(r,0) = \frac{1}{\eta_1}\left(\frac{\partial p}{\partial z}\right)_{t=0}. \quad \text{A.1}$$

It can be written as

$$\nabla^2\left(\nabla^2 - \frac{\mu}{\eta_1}\right) w(r,0) = \frac{1}{\eta_1}\left(\frac{\partial p}{\partial z}\right)_{t=0}. \quad \text{A.2}$$

Let $$V = \left(\nabla^2 - \frac{\mu}{\eta_1}\right) w(r,0) \quad \text{A.3}$$

Then, A.2 becomes

$$\nabla^2 V = \frac{1}{\eta_1}\left(\frac{\partial p}{\partial z}\right)_{t=0}, \quad \text{A.4}$$

or

$$\frac{\partial^2 V}{\partial r^2} + \frac{1}{r}\frac{\partial V}{\partial r} = \frac{1}{\eta_1}\left(\frac{\partial p}{\partial z}\right)_{t=0}. \quad \text{A.5}$$

This equation can be re-written as:

$$r^2\frac{\partial^2 V}{\partial r^2} + r\frac{\partial V}{\partial r} = r^2\frac{1}{\eta_1}\left(\frac{\partial p}{\partial z}\right)_{t=0}, \quad \text{A.6}$$

which is a Cauchy-Euler equation of order 2.

Thus, the complementary function is $$V_c(r) = c_1 + c_2 \ln r. \quad \text{A.7}$$

Assume the particular integral to be $$V_p(r) = Ar^2 + Br + D \quad \text{A.8}$$

Substituting the expression in A.8 in A.6 and comparing the coefficients of different powers of r, we get

$$A=\frac{1}{4\eta_1}\left(\frac{\partial p}{\partial z}\right)_{t=0},\ B=0. \qquad \text{A.9}$$

Thus, the general solution of equation (A.6) is

$$V(r)=V_c(r)+V_g(r),$$

$$=c_1+c_2\ln r+\frac{1}{4\eta_1}\left(\frac{\partial p}{\partial z}\right)_{t=0}r^2, \qquad \text{A.10}$$

(the constant D in A.8 is absorbed in c_1) .

In view of the boundary conditions (iii) and (iv) in (13), $c_2=0$.

Using A.10 in Equation A.3, we get

$$\left(\nabla^2-\frac{\mu}{\eta_1}\right)w(r,0)=c_1+\frac{1}{4\eta_1}\left(\frac{\partial p}{\partial z}\right)_{t=0}r^2, \qquad \text{A.11}$$

which can be written as

$$r^2\frac{\partial^2}{\partial r^2}w(r,0)+r\frac{\partial}{\partial r}w(r,0)-\frac{\mu}{\eta_1}r^2w(r,0)=c_1r^2+\frac{1}{4\eta_1}\left(\frac{\partial p}{\partial z}\right)_{t=0}r^4. \qquad \text{A.12}$$

The complementary function is

$$w_c(r)=d_1I_0\left(\sqrt{\frac{\mu}{\eta_1}}r\right)+d_2K_0\left(\sqrt{\frac{\mu}{\eta_1}}r\right). \qquad \text{A.13}$$

where $I_0\left(\sqrt{\frac{\mu}{\eta_1}}r\right)$ and $K_0\left(\sqrt{\frac{\mu}{\eta_1}}r\right)$ are the modified Bessel functions of the first and second kind, respectively.

Assume the Particular integral as $w_p=A_0r^4+B_0r^3+C_0r^2+D_0r+E_0$. A.14

Substituting the expression A.14 in A.12 and comparing the coefficients of different powers of ξ, we get

$$w_p=-\frac{1}{4\eta_1}\left(\frac{\partial p}{\partial z}\right)_{t=0}r^2-\frac{\eta_1}{\mu^2}\left(\frac{\partial p}{\partial z}\right)_{t=0}-\frac{\eta_1}{\mu}c_1. \qquad \text{A.15}$$

Thus,

$$w(r,0)=d_1I_0\left(\sqrt{\frac{\mu}{\eta_1}}r\right)+d_2K_0\left(\sqrt{\frac{\mu}{\eta_1}}r\right)-\frac{1}{4\mu}\left(\frac{\partial p}{\partial z}\right)_{t=0}r^2-\frac{\eta_1}{\mu^2}\left(\frac{\partial p}{\partial z}\right)_{t=0}-\frac{\eta_1}{\mu}c_1. \qquad \text{A.16}$$

(In view of the boundary conditions (iii) and (iv) in expression (13))

Since the derivative of $K_0(r)$ at $r=0$ is infinite, d_2 is to be taken zero.

Thus,

$$w(r,0)=d_1I_0\left(\sqrt{\frac{\mu}{\eta_1}}r\right)-\frac{1}{4\eta_1}\left(\frac{\partial p}{\partial z}\right)_{t=0}r^2-\frac{\eta_1}{\mu^2}\left(\frac{\partial p}{\partial z}\right)_{t=0}-\frac{\eta_1}{\mu}c_1. \qquad \text{A.17}$$

Using the boundary conditions (i) and (ii) in expression (13) (when $p_{tr}(z)=0$)in section 2, we get

$$d_1=\frac{\frac{1}{2\mu}\left(\frac{\partial p}{\partial z}\right)_{t=0}(1-\sigma)}{\frac{\mu}{\eta_1}I_0''\left(\sqrt{\frac{\mu}{\eta_1}}r\right)-\sigma\sqrt{\frac{\mu}{\eta_1}}I_0'\left(\sqrt{\frac{\mu}{\eta_1}}r\right)}, \qquad \text{A.18}$$

and

$$\frac{\eta_1}{\mu}c_1=-\frac{\eta_1}{\mu^2}\left(\frac{\partial p}{\partial z}\right)_{t=0}-\frac{1}{4\mu}\left(\frac{\partial p}{\partial z}\right)_{t=0}(R_0)^2+\frac{\frac{1}{2\mu}\left(\frac{\partial p}{\partial z}\right)(1-\sigma)I_0\left(\sqrt{\frac{\mu}{\eta_1}}R_0\right)}{\frac{\mu}{\eta_1}I_0''\left(\sqrt{\frac{\mu}{\eta_1}}R_0\right)-\frac{\sigma}{R_0}\sqrt{\frac{\mu}{\eta_1}}I_0'\left(\sqrt{\frac{\mu}{\eta_1}}R_0\right)}. \qquad \text{A.19}$$

Substituting A.18 and A.19 in A.17, we get the expression (17) in section 2.